

Potential energy curves using unrestricted Møller–Plesset perturbation theory with spin annihilation

H. Bernhard Schlegel^{a)}

Department of Chemistry, Wayne State University, Detroit, Michigan 48202

(Received 11 September 1985; accepted 14 January 1986)

Unrestricted Hartree–Fock and unrestricted Møller–Plesset perturbation theory are convenient methods to compute potential energy curves for bond dissociation, since these methods approach the correct dissociation limit. Unfortunately, a spin unrestricted wave function can contain large contributions from unwanted spin states that can distort the potential energy surface significantly. The spin contamination can be removed by projection or annihilation operators. As is well known, the spin project unrestricted Hartree–Fock bond dissociation curves have a large kink at the onset of the UHF/RHF instability, and a spurious minimum just beyond. However, the spurious minimum disappears and the kink is very much less pronounced at the unrestricted Møller–Plesset level with spin projection. Bond dissociation potentials for LiH and CH₄ were computed at the fourth order Møller–Plesset level plus spin projection,⁴ and good agreement was found with full CI and MR-CISD calculations.

INTRODUCTION

The unrestricted Hartree–Fock (UHF) method enjoys widespread usage for several reasons. It is a convenient approach for open shell systems, since acceptable spin densities can be obtained with a single determinantal formalism. There are also advantages for the calculation of energy surfaces, since bond dissociation curves are often qualitatively correct at the UHF level.¹ In many studies it is necessary to include an estimate of electron correlation energy. For larger systems, perturbational methods may be more practical than configuration interaction for calculating electron correlation. Because the UHF wave function is single determinantal and obeys Brillouin's theorem, the computation of correlation energy by many body perturbation theory (MBPT) or Møller–Plesset perturbation theory (MPn) is not significantly more difficult than for closed shell restricted wave functions.⁶

The major shortcoming of the UHF method is that the wave functions are not eigenfunctions of \hat{S}^2 . Frequently this is not a problem, since the contamination from higher spin states is often small. However, there are circumstances where the spin contamination can be large enough to adversely effect the shape of the energy surface and the magnitude of the spin densities. Such situations occur when, in a restricted Hartree–Fock treatment, occupied and unoccupied orbitals become nearly degenerate. For example, when a single bond is stretched to dissociation, the separation between bonding and antibonding orbitals approaches zero and the wave function tends to an equal mixture of singlet and triplet states. Another case is the twisting of ethylene, where the π and π^* orbitals become equivalent by symmetry at the transition state for rotation about the double bond. It should be noted (see below) that the spin contamination in UHF wave functions is not reduced significantly by perturbational corrections for electron correlation. Furthermore,

perturbation theory may be very slow to converge for large spin contamination.²

A number of approaches have been used to remedy the spin contamination problem: restricted open shell Hartree–Fock (ROHF), spin extended Hartree–Fock^{7,8} (EHF), spin projected unrestricted Hartree–Fock^{7,9} (PUHF), and multiconfiguration self-consistent field (MCSCF). The first two are desirable because the wave functions are monodeterminantal and easy to interpret, but adding perturbative corrections for electron correlation is difficult. Many body perturbation theory is more complex for ROHF¹⁰ than for UHF, but more importantly it is very slow to converge when occupied and unoccupied orbitals are nearly degenerate. Thus, configuration interaction is preferable to perturbation theory to improve ROHF wave functions. The spin extended Hartree–Fock approach (EHF) uses an effective Hamiltonian with three and four particle operators;¹¹ thus perturbation theory is rather difficult even for low orders. Spin projected unrestricted Hartree–Fock is also not without problems. The PUHF potential energy curves for bond dissociation have a very pronounced kink (discontinuity in the first derivative) where the restricted Hartree–Fock wave function becomes unstable relative to the unrestricted.¹² The MCSCF approach is perhaps the best choice, but is currently limited to smaller systems than UHF calculations and corrections for dynamic correlation are more difficult.

The purpose of this note is to apply spin projection to UHF and Møller–Plesset perturbation theory calculations to obtain improved potential energy curves. The effectiveness of annihilating the largest spin contaminant is tested on a few simple bond dissociation potential energy curves computed at the UHF and MPn levels.

FORMALISM

In the UHF approach, the wave function for an n electron system can be written

$$\Phi_0 = A(\phi_1 \cdots \phi_i \cdots \phi_{n_\alpha} \bar{\phi}_1 \cdots \bar{\phi}_1 \cdots \bar{\phi}_{n_\beta}),$$
$$n = n_\alpha + n_\beta, \quad s_z = 1/2 |n_\alpha - n_\beta|, \quad (1)$$

^{a)} Camille and Henry Dreyfus Teacher–Scholar.

where ϕ_i and $\bar{\phi}_j$ are α and β spin orbitals, respectively. The operator for \hat{S}^2 can be written in terms of operators for the individual electrons.

$$\hat{S}^2 = \hat{S}_z^2 + \hat{S}_z + \hat{S}_- \hat{S}_+, \quad (2)$$

$$\hat{S}_z = \sum_i \hat{s}_z(i), \quad \hat{S}_\pm = \sum_i \hat{s}_\pm(i). \quad (3)$$

Thus, \hat{S}^2 is a two electron operator

$$\hat{S}^2 = \left[\sum_i \hat{s}_z(i) \right] \left[\sum_i \hat{s}_z(i) \right] + \sum_i \hat{s}_z(i) + \sum_i \hat{s}_-(i) \hat{s}_+(i) + \sum_{i \neq j} \hat{s}_-(i) \hat{s}_+(j). \quad (4)$$

The UHF orbitals are eigenfunctions of \hat{s}_z but not of \hat{s}_\pm :

$$\begin{aligned} \hat{s}_z \phi_i &= \frac{1}{2} \phi_i, & \hat{s}_z \bar{\phi}_j &= -\frac{1}{2} \bar{\phi}_j, \\ \hat{s}_+ \phi_i &= 0, & \hat{s}_+ \bar{\phi}_j &= \sum_i S_{ij} \phi_i, \\ \hat{s}_- \phi_i &= \sum_j S_{ij} \bar{\phi}_j, & \hat{s}_- \bar{\phi}_j &= 0, \end{aligned} \quad (5)$$

where

$$S_{ij} = \int \phi_i \hat{s}_+ \bar{\phi}_j d\tau \quad (6)$$

(i.e., overlap between spatial parts of the α and β orbitals). Thus, the expectation value for \hat{S}^2 for a UHF wave function is

$$\langle S^2 \rangle_0 = \langle \Phi_0 | \hat{S}^2 | \Phi_0 \rangle = s_z^2 + s_z + n_\beta - \sum_{ij} S_{ij}. \quad (7)$$

Using the Møller–Plesset perturbation theory to estimate electron correlation energy, the first and second order corrections to the wave function are

$$\Phi_1 = - \sum_i \{ \psi_i \langle \psi_i | \hat{V} | \Phi_0 \rangle / (E_i - E_0) \}, \quad (8)$$

$$\Phi_2 = \sum_i \left\{ \psi_i \left(\sum_j \frac{\langle \psi_i | \hat{V} | \psi_j \rangle \langle \psi_j | \hat{V} | \Phi_0 \rangle}{(E_i - E_0)(E_j - E_0)} - \frac{E_1 \langle \psi_i | \hat{V} | \Phi_0 \rangle}{(E_i - E_0)^2} \right) \right\}, \quad (9)$$

where $V = H - F$ (F is the unrestricted Fock operator) and where Φ_1 involves only double excitations, while Φ_2 contains single, double, triple, and quadruple excitations. The expectation values of \hat{S}^2 correct to first and second order are

$$\langle \hat{S}^2 \rangle_1 = \langle \hat{S}^2 \rangle_0 + 2 \langle \Phi_0 | \hat{S}^2 | \Phi_1 \rangle, \quad (10)$$

$$\begin{aligned} \langle S^2 \rangle_2 &= \langle S^2 \rangle_1 + 2 \langle \Phi_0 | \hat{S}^2 | \Phi_2 \rangle + \langle \Phi_1 | \hat{S}^2 | \Phi_1 \rangle \\ &\quad - \langle S^2 \rangle_0 \langle \Phi_1 | \Phi_1 \rangle. \end{aligned} \quad (11)$$

Neither the UHF wave function Φ_0 nor the correlation corrections Φ_1 , Φ_2 , etc. are eigenfunctions of \hat{S}^2 . At any finite order of perturbation theory the wave function is a mixture of the desired spin state and unwanted states of different spin.

One method to remove the spin contamination in spin unrestricted wave functions is to use projection or annihilation operators.⁷ The projection or annihilation can be done before, during, or after the perturbation calculations for electron correlation. If the projection is done first, higher excitations enter even in low orders of perturbation theory and it is probably more practical to start with an ROHF wave function. Projection could be carried out during the perturbation calculations for electron correlation by including spin projection as an additional perturbation, however this is somewhat complicated to formulate. By comparison spin annihilation after the perturbation corrections for electron correlation is relatively straightforward.

The Löwdin spin projection operator can be written⁷

$$\hat{P}_s = \prod_{l \neq s} \frac{\hat{S}^2 - l(l+1)}{s(s+1) - l(l+1)}. \quad (12)$$

For a spin free Hamiltonian, the variational energy can then be written

$$\begin{aligned} E_{\text{proj}} &= \langle \hat{P}_s \Phi_0 | \hat{H} | \hat{P}_s \Phi_0 \rangle / \langle \hat{P}_s \Phi_0 | \hat{P}_s \Phi_0 \rangle, \\ &= \langle \Phi_0 | \hat{H} \hat{P}_s | \Phi_0 \rangle / \langle \Phi_0 | \hat{P}_s | \Phi_0 \rangle. \end{aligned} \quad (13)$$

Often, the largest contribution to the spin contamination in a UHF calculation comes from the next highest spin multiplicity.¹³ Under such circumstances the full spin projection operator can be approximated quite well by an operator that annihilates only the next highest spin,^{9,14,15}

$$\hat{P}_s \Phi_0 \simeq \hat{A}_{s+1} \Phi_0 = \frac{\hat{S}^2 - (s+1)(s+2)}{\langle \hat{S}^2 \rangle_0 - (s+1)(s+2)} \Phi_0. \quad (14)$$

The particular choice of the denominator assures normalization of Φ_0 (i.e., $\langle \Phi_0 | \hat{A}_{s+1} \Phi_0 \rangle = 1$, intermediate normalization). This can be expanded in terms of singly and doubly excited determinants.

$$\begin{aligned} \hat{A}_{s+1} \Phi_0 &= \Phi_0 + \sum_i \frac{\langle \psi_i | \hat{S}^2 | \Phi_0 \rangle \psi_i}{\langle \hat{S}^2 \rangle_0 - (s+1)(s+2)} \\ &= \Phi_0 + \tilde{\Phi}_1. \end{aligned} \quad (15)$$

Thus, the correction to ϕ_0 due to spin projection $\tilde{\phi}_1$ can be considered to belong to the same order of perturbation as ϕ_1 .

The Hartree–Fock energy after single annihilation of the next highest spin is given by

$$\begin{aligned} \langle \Phi_0 | \hat{H} | \hat{A}_{s+1} \Phi_0 \rangle &= \langle \Phi_0 | \hat{H} | \Phi_0 + \tilde{\Phi}_1 \rangle = E_{\text{HF}} + \langle \Phi_0 | \hat{V} | \tilde{\Phi}_1 \rangle \\ &= E_{\text{HF}} + \sum_i \frac{\langle \Phi_0 | \hat{V} | \psi_i \rangle \langle \psi_i | \hat{S}^2 | \Phi_0 \rangle}{\langle \hat{S}^2 \rangle_0 - (s+1)(s+2)}. \end{aligned} \quad (16)$$

When the corrections for electron correlation are added, Φ_1 , Φ_2 , etc., the correction for spin projection $\tilde{\Phi}_1$ must be reduced by the amount already contained in Φ_1 , Φ_2 , etc.

$$\begin{aligned} \tilde{\Phi}_1 &= \tilde{\Phi}_1 \left(1 - \frac{\langle \tilde{\Phi}_1 | \Phi_1 + \Phi_2 \dots \rangle}{\langle \tilde{\Phi}_1 | \tilde{\Phi}_1 \rangle} \right) \\ &= \sum_i \frac{\psi_i \langle \psi_i | \hat{S}^2 | \Phi_0 \rangle}{\langle \hat{S}^2 \rangle_0 + (s+1)(s+2)} \left\{ 1 - \frac{\langle \Phi_0 | S^2 | \Phi_1 + \Phi_2 \rangle [\langle \hat{S}^2 \rangle_0 - (s+1)(s+2)]}{\sum_i \langle \Phi_0 | \hat{S}^2 | \psi_i \rangle^2} \right\}. \end{aligned} \quad (17)$$

TABLE I. Correlation corrections to $\langle S^2 \rangle$ for LiH as a function of bond length.

R^a	$\langle S^2 \rangle_0$	$\langle S^2 \rangle_1$	$\langle S^2 \rangle_2$
2.0334 ^b	0	0	0
2.15	0.346 35	0.298 29	0.228 05
2.25	0.523 03	0.468 12	0.390 85
2.35	0.642 88	0.590 69	0.520 01
2.50	0.761 36	0.718 31	0.663 01
2.75	0.871 79	0.843 86	0.816 30
3.00	0.928 72	0.911 55	0.891 92
3.50	0.977 34	0.971 34	0.964 79
4.00	0.992 97	0.991 04	0.988 91
5.00	0.999 44	0.999 29	0.999 12

^a Bond lengths in Å.^b Onset of UHF-RHF instability.

The remaining spin contamination in Φ_1, Φ_2, Φ_3 , etc., can be projected in a similar fashion. However, the component belonging to $\tilde{\Phi}_1$ must be removed first:

$$\Phi'_1 = \Phi_1 - \tilde{\Phi}_1 \langle \tilde{\Phi}_1 | \Phi_1 \rangle / \langle \tilde{\Phi}_1 | \tilde{\Phi}_1 \rangle$$

(likewise for Φ'_2, Φ'_3 , etc.),

$$\hat{A}_{s+1} \Phi'_1 = \Phi'_1 + \tilde{\Phi}_2. \quad (18)$$

The spin correction term $\tilde{\Phi}_2$ must be reduced by the amount already contained in Φ_2, Φ_3 , etc.,

$$\tilde{\Phi}'_2 = \tilde{\Phi}_2 (1 - \langle \tilde{\Phi}_2 | \Phi'_2 \dots \rangle / \langle \tilde{\Phi}_2 | \tilde{\Phi}_2 \rangle). \quad (19)$$

Like Φ_2 , $\tilde{\Phi}'_2$ contains single, double, triple, and quadruple excitations.

If the total energy for the unprojected wave function is written

$$E = \langle \Phi_0 | \hat{H} | \Phi_0 + \Phi_1 + \Phi_2 + \Phi_3 \dots \rangle \\ = E_{\text{HF}} + E_2 + E_3 + E_4 \dots, \quad (20)$$

then the energy after spin annihilation is given by

$$E_{\text{proj}} = \langle \Phi_0 | \hat{H} | \Phi_0 + \Phi_1 + \tilde{\Phi}'_1 + \Phi_2 + \tilde{\Phi}'_2 + \Phi_3 \dots \rangle. \quad (21)$$

As will be seen below, Φ_1 changes the expectation value

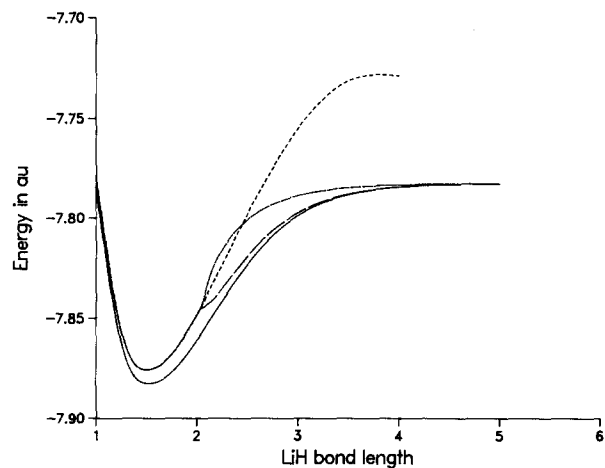


FIG. 2. Comparison of LiH bond dissociation potentials: restricted MP2 (short dash), unrestricted MP2 (medium dash), projected unrestricted MP2 (long dash), and full CI (solid).

of \hat{S}^2 by only a small amount, and higher corrections by even less. Thus, the projection of Φ_1, Φ_2 , etc., can be expected to change by energy by a much smaller amount than the projection of Φ_0 . These corrections and other refinements will be considered in a subsequent paper. In the present application, the following are used to estimate the spin projected second, third, and fourth order Møller-Plesset energies:

$$\Delta E_{\text{PUHF}} = \sum_i \langle \Phi_0 | \hat{V} | \psi_i \rangle \langle \psi_i | \hat{S}^2 | \Phi_0 \rangle / \\ [\langle \hat{S}^2 \rangle_0 - (s+1)(s+2)], \quad (22)$$

$$E_{\text{PUHF}} = E_{\text{HF}} + \Delta E_{\text{PUHF}}, \quad (23)$$

$$E_{\text{PMP2}} \simeq E'_{\text{PMP2}} \\ = E_{\text{MP2}} + \Delta E_{\text{PUHF}} (1 - \langle \tilde{\Phi}_1 | \Phi_1 \rangle / \langle \tilde{\Phi}_1 | \tilde{\Phi}_1 \rangle), \quad (24)$$

$$E_{\text{PMP3}} \simeq E'_{\text{PMP3}} \\ = E_{\text{MP3}} + \Delta E_{\text{PUHF}} (1 - \langle \tilde{\Phi}_1 | \Phi_1 + \Phi_2 \rangle / \langle \tilde{\Phi}_1 | \tilde{\Phi}_1 \rangle), \quad (25)$$

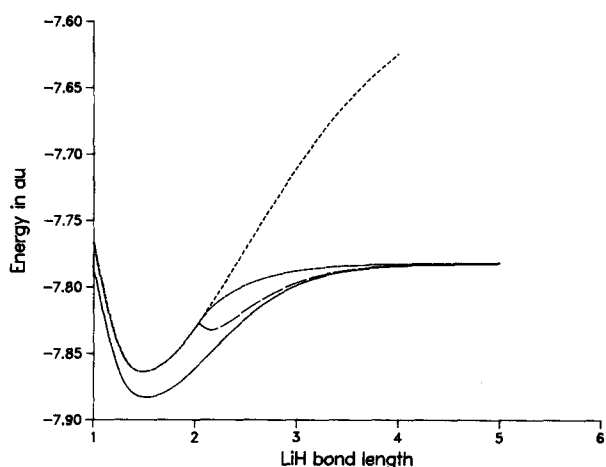


FIG. 1. Comparison of LiH bond dissociation potentials: RHF (short dash), UHF (medium dash), projected UHF (long dash), and full CI (solid).

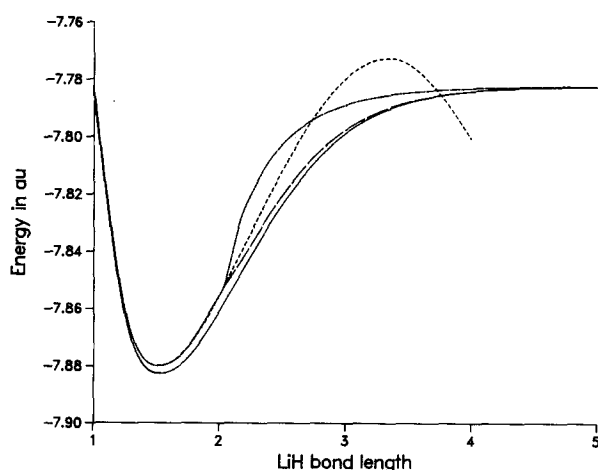


FIG. 3. Comparison of LiH bond dissociation potentials: restricted MP3 (short dash), unrestricted MP3 (medium dash), projected unrestricted MP3 (long dash), and full CI (solid).

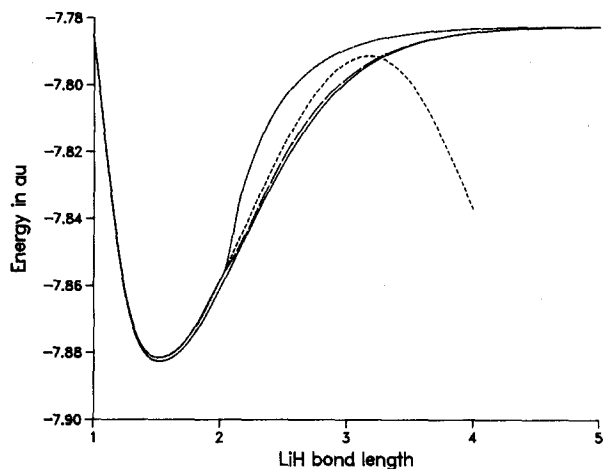


FIG. 4. Comparison of LiH bond dissociation potentials: restricted MP4SDTQ (short dash), unrestricted MP4SDTQ (medium dash), projected unrestricted MP4SDTQ (long dash), and full CI (solid).

$$\begin{aligned}
 E_{\text{PMP4}} &\approx E'_{\text{PMP4}} \\
 &= E_{\text{MP4}} + \Delta E_{\text{PUHF}} (1 - \langle \tilde{\Phi}_1 | \Phi_1 + \Phi_2 + \Phi_3 \rangle / \\
 &\quad \langle \tilde{\Phi}_1 | \tilde{\Phi}_1 \rangle), \\
 E''_{\text{PMP4}} &\approx E_4 + E'_{\text{PMP3}}.
 \end{aligned} \quad (26)$$

DISCUSSION

The formalism outlined above was tested in a series of simple calculations of the LiH bond dissociation potential. Energies were computed at the restricted and unrestricted HF, MP2, and MP3 and MP4SDTQ levels with and without spin annihilation using a minimal basis set (1s, 2s, 2p_x, 2p_y, 2p_z, on Li; 1s on H). Table I shows $\langle S^2 \rangle$ at various bond lengths. It is clear that perturbational corrections for electron correlation do not reduce the spin contamination significantly.¹⁶ After annihilation of the next highest spin, $\langle S^2 \rangle$ can be computed by $\langle \Phi_0 | \hat{S}^2 | \hat{A}_{s+1} \Phi_0 \rangle$ or $\langle \hat{A}_{s+1} \Phi_0 | \hat{S}^2 | \hat{A}_{s+1} \Phi_0 \rangle / \langle \hat{A}_{s+1} \Phi_0 | \hat{A}_{s+1} \Phi_0 \rangle$. At $R = 3 \text{ \AA}$, both values are 0.0000, indicating that annihilation of only $s + 1$ is a very good approximation for LiH at intermediate bond lengths.

Figures 1–4 compare the restricted, unrestricted, and projected HF, MP2, MP3, and MP4 results to the full CI

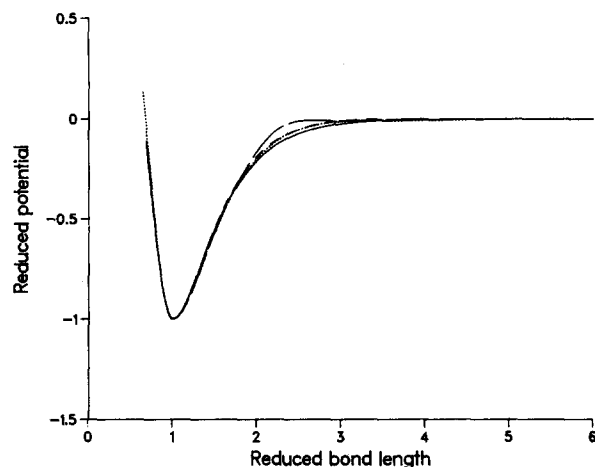


FIG. 5. Comparison of the reduced potentials for CH bond dissociation in CH₄ along the minimum energy path: MP4 (long dash), projected MP4 (short dash), Brown and Truhlar MR-CISD (dotted), and Morse (solid).

(i.e., exact within the minimal basis). The following well known facts¹² can be observed from Fig. 1: (a) The RHF curve goes to the wrong limit; (b) the UHF goes to the correct limit; (c) the PUHF curve has a discontinuity in slope at the onset of the UHF–RHF instability, and a spurious minimum just beyond. Similarly, some aspects of Figs. 2–4 are well known: (a) Perturbation theory breaks down for RMP2, RMP3, and RMP4 as the bond is extended; (b) the UMP2, UMP3, and UMP4 curves go to the right limit but are too high in the intermediate region. There are, however, some features that have not been discussed previously. The spurious minimum found at the PUHF level disappears when electron correlation is added. In addition, the kink becomes much less pronounced at higher levels of perturbation. The agreement with the exact curve is very good at fourth order. Both higher order perturbation theory and more complete treatment of spin projection would improve the agreement further.

The second example is the CH dissociation potential for CH₄ studied previously.⁴ Computation was carried out¹⁸ at the MP4SDTQ/6-31G** level, with and without annihilation of the largest spin contaminant. The geometries, energies, and expectation values of \hat{S}^2 are given in Table II. It is again evident from the values of $\langle S^2 \rangle$ that the perturbation corrections for electron correlation do not remedy the spin

TABLE II. C–H bond dissociation potential for CH₄^a.

R	θ	$\langle S^2 \rangle_0$	$\langle S^2 \rangle_1$	$\langle S^2 \rangle_2$	E_{MP4}	E''_{PMP4}
0.757	111.33 ^b	0	0	0	–40.248 933	
1.086	109.47 ^b	0	0	0	–40.393 846	
1.500	105.72 ^b	0	0	0	–40.340 360	
2.000	100.57 ^c	0.660 36	0.601 32	0.515 65	–40.246 086	–40.272 271
2.500	96.47 ^c	0.928 13	0.901 87	0.871 23	–40.224 104	–40.241 580
3.000	91.30 ^c	0.992 79	0.979 81	0.968 65	–40.219 059	–40.230 559
4.000	90.0 ^c	1.011 0	1.002 4	1.997 63	–40.217 727	–40.227 036
10.00	90.0 ^c	1.011 8	1.003 5	1.998 99	–40.217 593	–40.226 797

^a Bond lengths in \AA , angles in deg, energies in a.u. (1 a.u. = 675.1 kcal/mol).

^b Spin restricted.

^c Unrestricted.

contamination problem. The improvement from first order to second order is particularly small. At a CH bond length of 2.5 Å, $\langle \Phi_0 | S^2 | \hat{A}_{s+1} \Phi_0 \rangle = -0.0337$ and $\langle \hat{A}_{s+1} \Phi_0 | S^2 | \hat{A}_{s+1} \Phi_0 \rangle / \langle \hat{A}_{s+1} \Phi_0 | \hat{A}_{s+1} \Phi_0 \rangle = +0.0667$, indicating that annihilation of only the triplet spin contaminant is adequate. However, there is a problem with size consistency, since the energy with spin annihilation for CH₄ at very large R (CH) is not the sum of the energies with spin annihilation for CH₃ and H. At the MP4 level, the difference is 4.6 kcal/mol. This is due to spin contamination in the UHF wave function for CH₃, and can be remedied by annihilating higher spins.

In Fig. 5 the present calculations are compared to a larger basis set MR-CISD calculation by Brown and Truhlar,¹⁹ and to a Morse curve fitted to the MP4 energies at $R = 1.086$, $R = 1.5$, and $R = \infty$. To facilitate comparison, the curves are plotted as reduced potentials, i.e., scaled so that $D_e = 1$ and $R_e = 1$. The MP4 curve is too high in the intermediate region because of the spin contamination. The spin projected MP4 and larger basis set MR-CISD curves are in very good agreement. Both are somewhat higher than the Morse curve. Thus, as stated previously,^{4,17} the correct potential energy curve lies between the unprojected MP4 and the Morse curve.

For the two examples treated, the approximate spin projected MP4 potential energy curves are in quite good agreement with the exact or very accurate calculations. Other applications include barriers for hydrogen atom addition to ethylene and formaldehyde,²⁰ and OH + C₂H₄ addition.²¹ The method is computationally simple and can be applied to larger molecules where full CI or large MR-CI are not feasible. However, unlike unprojected Møller–Plesset perturbation theory and full spin projection, energies obtained by annihilating only the next highest spin are not size consistent.

ACKNOWLEDGMENTS

This work was supported by a grant from the National Science Foundation (Grant No. CHE-83-12505). The au-

thor wishes to thank Dr. J. A. Pople for helpful discussions and M. A. Robb for use of his MCSCF program for the full CI calculations.

¹Energy surfaces and the breaking of spatial and spin symmetries have been discussed in detail by H. Fukutome, *Int. J. Quantum Chem.* **20**, 955 (1981). For some examples of bond dissociation potentials calculated with UHF and unrestricted Møller–Plesset perturbation theory compared to other methods, see Refs. 2–5.

²N. C. Handy, P. J. Knowles, and K. Somasundram, *Theor. Chim. Acta* **68**, 87 (1985).

³R. J. Bartlett and G. D. Purvis III, *Phys. Scr.* **21**, 255 (1980).

⁴R. J. Duchovic, W. L. Hase, H. B. Schlegel, M. J. Frisch, and K. Raghavachari, *Chem. Phys. Lett.* **89**, 120 (1982).

⁵M. R. Nyden and G. A. Petersson, *J. Chem. Phys.* **74**, 6312 (1981); J. Tino and V. Klimo, *Int. J. Quantum Chem.* **10**, 761 (1976); V. Klimo and J. Tino, *Mol. Phys.* **35**, 1771 (1978); **41**, 483 (1980); **46**, 541 (1982); *Int. J. Quantum Chem.* **25**, 733 (1984).

⁶R. J. Bartlett, *Annu. Rev. Phys. Chem.* **32**, 359 (1981).

⁷P. -O. Löwdin, *Phys. Rev.* **97**, 1509 (1955).

⁸For a recent review of the spin projected extended Hartree–Fock methods, see I. Mayer, *Adv. Quantum. Chem.* **12**, 189 (1980).

⁹T. Amos and G. G. Hall, *Proc. R. Soc. London Ser. A* **263**, 483 (1961).

¹⁰I. Hubac and P. Carsky, *Phys. Rev. A* **22**, 2392 (1980).

¹¹S. Biskrusic and V. Kvasnicka, *Int. J. Quantum. Chem.* **21**, 633 (1982).

¹²See, for example, I. Mayer, *Int. J. Quantum. Chem.* **14**, 29 (1978).

¹³The situation is more complicated if more than one electron pair is involved (e.g., stretching two single bonds or breaking multiple bonds).

¹⁴P. J. Rossky and M. Karplus, *J. Chem. Phys.* **73**, 6196 (1980).

¹⁵Using a perturbational expansion of the UHF wave function, it has been shown (Ref. 14) that the total energy obtained with the full projector and with a single annihilator are the same through third order.

¹⁶Coupled cluster methods appear to be better at reducing spin contamination, though the number of iterations required to solve the coupled cluster equations may increase significantly for large spin contamination (see Ref. 17).

¹⁷R. J. Bartlett, H. Sekino, and G. D. Purvis III, *Chem. Phys. Lett.* **98**, 66 (1983); H. Sekino and R. J. Bartlett, *J. Chem. Phys.* **82**, 4225 (1985).

¹⁸J. S. Binkley, R. A. Whiteside, R. Krishnan, R. Seeger, D. J. DeFrees, H. B. Schlegel, S. Topiol, L. R. Kahn, and J. A. Pople, *QCPE* **13**, 406 (1980) and more recent releases from Carnegie Mellon University, Pittsburgh, Pennsylvania.

¹⁹F. B. Brown and D. G. Truhlar, *Chem. Phys. Lett.* **113**, 441 (1985).

²⁰C. Sosa and H. B. Schlegel, *Int. J. Quantum Chem.* (to be published).

²¹C. Sosa and H. B. Schlegel (in preparation).